Research Article

Wanzhi Ma and Na Chu*

Evaluation of online teaching quality in colleges and universities based on digital monitoring technology

https://doi.org/10.1515/jisys-2023-0312
received December 15, 2023; accepted March 11, 2024

Abstract: The intelligent university teaching detection system can effectively improve the teaching efficiency of university classrooms and improve the teaching environment. In order to improve the quality of online teaching supervision, this study combines digital monitoring technology to monitor the online teaching process in colleges and universities, and analyzes the method and process of using the equivalence line and the rotation theorem to estimate the projection angle. This work applies a projection method to digital teaching detection, improves the algorithm based on requirements, uses factor improvement methods to improve the problems in model application, uses requirement analysis methods to construct a system model, and uses experimental analysis methods to verify the effectiveness of the proposed algorithm and model. With the support of simulation platforms and mathematical statistical methods, the effectiveness of the system model is verified in this work. From the evaluation results, it can be seen that the evaluation results of the system model in this work are distributed between [84,92], indicating that the use of the system in this study is very excellent. The experimental research shows that the digital online monitoring technology proposed in this study can monitor students in real time in online teaching in colleges and universities, effectively improve the participation of students in the online teaching process, and play an important role in improving the quality of teaching.

Keywords: digital monitoring, colleges and universities, online teaching, quality evaluation

1 Introduction

Currently, some experts and scholars are researching the application of digital monitoring technology in teaching environment monitoring, using digital monitoring technology to identify the teaching environment and the status of teachers and students, providing some auxiliary information for the teaching process, and promoting the effective implementation of teaching activities [1].

There are three main sources of digital teaching resources for environmental monitoring technology courses: digital transformation of existing teaching resources; electronic works created by teachers and students, including skills competition process and finished materials; resources developed and constructed by professionals. Among them, there are three basic types of electronic works created by teachers and students, namely, exhibition works, collections of communication between teachers and students, and collections of works for teachers to evaluate students. The resources developed and constructed by professionals are

* **Corresponding author: Na Chu**, School of Foreign Languages, Ningxia Normal University, Guyuan Ningxia, 756099, China, e-mail: 82007063@nxnu.edu.cn
Wanzhi Ma: School of Educational Science, Ningxia Normal University, Guyuan Ningxia, 756099, China, e-mail: mawanzhi79@nxnu.edu.cn

Open Access. © 2024 the author(s), published by De Gruyter. This work is licensed under the Creative Commons Attribution 4.0 International License.

the main sources of digital teaching resources. The development and construction steps are as follows: collect various forms of media materials, and classify and describe the materials; integrate various scattered materials into a complete teaching resource unit; indexing of resource content; quality inspection; after the completion of resource production, all digital files need to be archived and stored in the resource library [2].

Intelligent teaching environment monitoring includes intelligent regulation of the environment in the teaching environment, temperature and humidity monitoring, lighting monitoring, student status monitoring, etc. The following is a summary of the existing research.

Intelligent environmental regulation is an air-conditioning control system composed of a central air-conditioning power controller, temperature and humidity sensors, and supporting control software. The temperature and humidity sensors are used to monitor the indoor temperature, and the background control system or pre-set reference values for the software transmit the monitoring data and analysis. When the indoor temperature and humidity are higher than the pre-set value, the air conditioner is automatically turned on to realize the automatic control of indoor temperature and humidity. With the continuous improvement of sensor technology, more and more indoor environmental parameter sensors are integrated into environmental quality monitoring instruments [3]. The indoor environmental monitoring parameters are extended from the original basic monitoring parameters such as PM2.5, TVOC, carbon dioxide, temperature, and humidity to PM10, formaldehyde, oxygen, ozone, carbon monoxide, nitrogen oxides, air pressure, light, noise, etc. The environmental monitoring system continuously obtains various environmental data in the classroom through the connected terminal monitoring equipment [4]. For abnormal conditions of different parameters, the system will send relevant information to managers, and managers can also actively view the monitoring data of each monitoring point. Through the long-term real-time monitoring of sensors, the environmental monitoring parameters in the classroom will always be kept within the appropriate intelligent range [5].

Intelligent lighting systems are usually dominated by automatic control, supplemented by manual control, and intelligent management and control are often required for lighting, electrical, and campus security in an intelligent teaching environment. In order to meet the requirements of lighting quality in different areas and realize different lighting control schemes, it is necessary to control and adjust the lighting intensity. The intelligent lighting management and control system will perform lighting work in a fully automatic state according to the preset basic state, and can also automatically switch between different states according to the pre-set time [6]. For example, after the end of the working day, the system will automatically enter the rest work state, adjust the lights in the detected manned areas to an appropriate brightness, and turn off the lights in the uninhabited areas. Because different scenes have different lighting requirements, the lighting in different areas can be changed through the Internet of Things (IoT) editor to suit different needs. Relying on the IoT platform, various hardware devices and software resources in the smart teaching system can be effectively coordinated, and linkage monitoring and automatic management and control can be realized through App control, remote control, and intelligent analysis control [7].

Traditional classrooms generally have low energy utilization efficiency. Due to the wide variety of various media equipment and complex equipment and facilities, management is difficult. Especially with the continuous introduction of a large number of new information technology media in the classroom, the energy wastage of machinery and equipment is becoming more and more serious [8]. With the help of IoT technology, smart classrooms can monitor the energy usage of various devices and solve the problem of energy wastage completely. The specific application of the IoT technology can be reflected in: first, energy consumption monitoring of various media equipment, mainly including real-time monitoring of energy consumption information in classrooms, historical data analysis of energy consumption information, and switch control of electrical appliances. The second is the measurement system of the smart environment, which mainly refers to the statistical analysis and real-time monitoring of broadband access management, wireless AP settings, network management testing, and value-added applications (such as network data sharing, classroom security management, etc.) [9]. Among the above two basic energy management, energy consumption is particularly important. How to use a reasonable energy consumption to maximize output has become an important factor restricting the promotion and application of smart classrooms in colleges and universities. At the same time, the use of network traffic is also worthy of in-depth study. With the help of wireless network coverage and logistics overall analysis and control in smart classrooms, information resources can be reasonably allocated and used optimally [10].

The digital campus network in universities is gradually advancing, and the number of network devices and servers is gradually increasing. The structure of the network is also becoming increasingly complex. It is crucial to have an intelligent management platform, and having a dynamically updated topology map is crucial for network management. The digital network monitoring platform of universities presents the network form in the form of WEB, and the network topology diagram is also very intuitive, making network management very convenient [11].

The digital network monitoring platform of universities can monitor devices and servers in the network environment in real time. If a device malfunctions, it can be reported through various methods in real time [12]. It can also dynamically see the running status of network devices and servers, and the running status of the devices can be dynamically displayed through topology maps and web pages. For complex faults that are not easy to maintain, the cause of the fault can be determined and resolved by searching the system logs. Therefore, any faults in the network can be resolved in a timely manner, ensuring the stable, safe, and effective operation of the digital network system in universities [13].

The network devices and servers in the digital campus network are important equipment for teaching activities in universities. Therefore, real-time monitoring of the operation status of the devices is necessary [14]. Adopting a modular programming approach, each module processes data in the network. The data are transmitted to the core or aggregation switch in the network through probes. Finally, by using real-time graphs and other methods on the management and monitoring platform, the monitored data are presented to individual managers, providing a basis for network managers to manage and maintain the network [15].

With the gradual advancement of digital campuses, the network scale of universities is becoming larger, and the number of devices and servers in the network is gradually increasing. The devices in the network are also relatively scattered, and the amount of maintenance work is increasing; after deploying the network management monitoring platform, the workload of network maintenance personnel is greatly reduced, thereby greatly reducing the cost of network maintenance.

With the gradual increase in the scale of university networks, the model and quantity of devices in the network have increased. There is no effective communication and management between devices from various manufacturers [16]. After using Simple Network Management Protocol (SNMP), communication between different vendors and devices can be easily managed, providing a basis for managing different hardware devices. The SNMP protocol is the most common protocol for network management devices, which is compatible with various network devices. Therefore, the campus network monitoring platform using the SNMP protocol can be seamlessly compatible with various new types of devices, achieving stable and dynamic upgrades of the platform [17].

With the development of digital construction in universities, the types and quantities of network equipment in universities are significantly increasing [18]. The traditional methods of network maintenance not only require a large amount of maintenance work but also have low reliability. Unable to adapt to the maintenance needs of the rapid development of the network [19], the university network monitoring platform based on SNMP protocol has changed the traditional network maintenance methods, allowing real-time control of the operation status of the campus network. Once a fault occurs, it can quickly locate and solve it, improving the management efficiency of the digital network, thereby ensuring the stable operation of the campus digital network system [20].

The organizational structure of this work is as follows: the first part is the introduction and literature review, which introduces the current problems of teaching quality evaluation in colleges and universities, summarizes the previous research, and introduces the research content of this work; the second part analyzes the algorithm of digital monitoring technology, the calibration algorithm of Euler angle γ and the projection image screening algorithm based on Euler angle and isoline are proposed, and the process of the projection image screening algorithm based on Euler angle and the algorithm for screening the equivalent line are analyzed. The third part is about the system. Finally, in the conclusion part, the research content of this study is summarized and prospected.

This work combines digital monitoring technology to monitor the online teaching process in colleges and universities, improves the effect of online teaching supervision in colleges and universities, improves the quality of online teaching, and eliminates the drawbacks brought by intelligent teaching reform to the teaching process.

Contributions of this study: In the process of image processing by traditional teaching monitoring algorithms, due to the low signal-to-noise ratio of the image or the existence of certain features, deviations occur in estimating the equivalence line, and these errors are gradually reduced with the calculation of the projection angle. Enlarged, the projection image screening algorithm based on Euler angles can filter out lower quality projection images, which also include projection images that are considered to be low quality due to inaccurate projection angle estimation. Therefore, in the future research, we can correct the projection angle of this part of the image, so this study can effectively improve the effect of online monitoring of college teaching.

The innovation of this article is as follows: Due to the influence of partial noise and erroneous features in teaching monitoring images, there is a significant error in the projection angle. The teaching monitoring projection image filtering algorithm proposed in this article can effectively filter out images with low quality and large projection angle errors, and only use some high-quality projection images to construct the initial model This article uses projection angle and equivalent line information to filter the projected image, thereby enhancing the initial model and making it closer to the real model in details. When iterating using the initial model, it can effectively avoid the deviation of the final 3D structure.

The purpose of this article is to use digital monitoring technology combined with intelligent 3D images for real-time recognition of student status in the teaching process of universities, providing more reliable teaching assistance information for teachers, and also providing technical support for the effective implementation of subsequent smart teaching models.

2 Methods

2.1 Image processing based on computational projection

The angle reconstruction algorithm mainly consists of two steps. The first is to use the normalized similarity to calculate the equivalent line between the projected graphics, and then use the three images and their equivalent lines to establish the Euler Cartesian coordinate system. The positions of all images in this coordinate system are relatively fixed. After that, the algorithm estimates the relative projection angle direction of all sample images by calculating the angle between the two images, and uses Euler angles α, β, and γ to represent the projection angles. The specific representation method is shown in Figure 1.

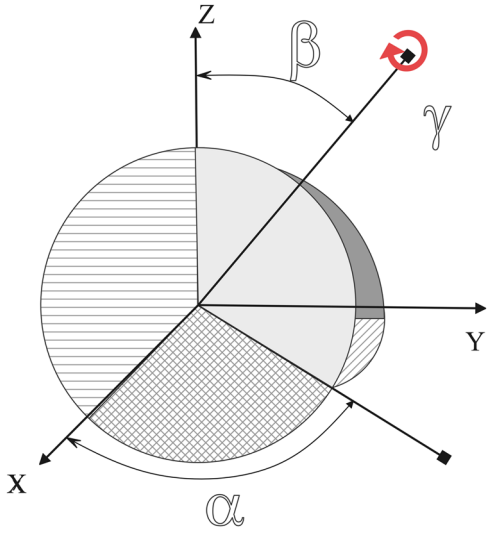

Figure 1: Euler angles α, β, and γ indicate the projection direction.

The α angle is the angle between the projection of the projection direction vector on the X–Y plane and the X axis; the β angle is the angle between the vector and the Z axis; the γ angle is the rotation angle of the image along the projection direction.

As shown in Figure 1, the angle reconstruction is also the basic principle of the algorithm proposed in this work to screen the projected image by calculating the Euler angle γ. The angle reconstruction algorithm divides the projection direction into three Euler angle variables, namely α, β, and γ, and then uses the information of the equivalence line to calculate these Euler angles respectively, which finally obtains the relative position of each image in the Fourier space.

If two 2D projection images with different projection directions come from the same 3D structure, then these two images also have the same equivalence line in the real number space. That is to say, in the three-dimensional coordinate system, two projection images of the same three-dimensional structure have an intersection line with exactly the same coordinates and values. The principle of the equivalent line is shown in Figure 2.

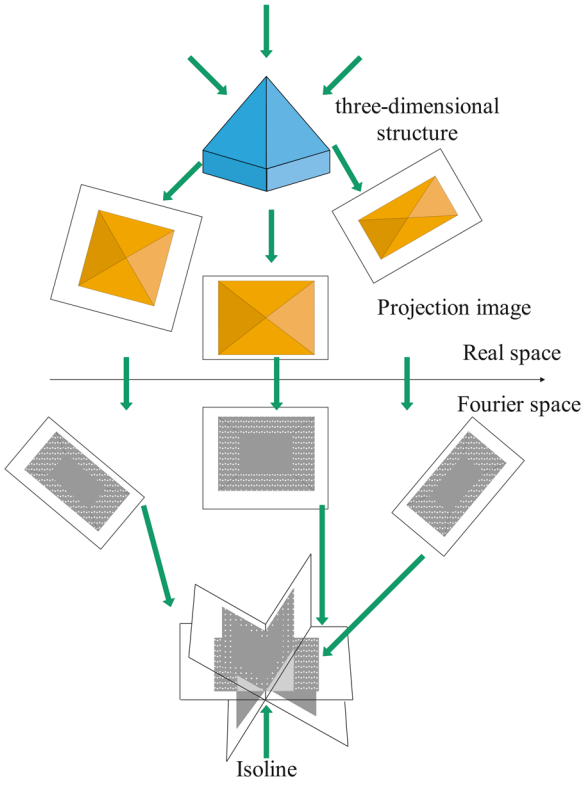

Figure 2: Schematic diagram of the equivalence line obtained by the central section theorem.

Before calculating the equivalent line of the image, the image data must be discretized, a certain degree is selected as the step size, and the distance from the positive half-axis of the X-axis as the starting point 0° to the end point 360° is discretized into several projection lines. Moreover, these discrete projection lines are rearranged in sequence to form a two-dimensional sinogram. In the same principle, we can also Fourier transform the projected image first, and then discretize it.

$$\Lambda_{kl} = \left\{\hat{P}_k\left(\frac{B}{n}, \frac{2\pi l}{L}\right), \hat{P}_k\left(\frac{2B}{n}, \frac{2\pi l}{L}\right), \ldots, \hat{P}_k\left(B, \frac{2\pi l}{L}\right)\right\}, \tag{1}$$

where $\hat{P}_k$ is the Fourier transform of the kth image. After discretization, the image is divided into n projection lines, and then the n lines are successively normalized for correlation calculation, and the maximum value among them is regarded as the equivalent line. The specific calculation formula is given as

$$(C(i,j), C(j,i)) = \underset{0\le S_1<L/2, 0s_2<L}{\arg\max} \frac{\langle \Lambda_{i,1_1}, \Lambda_{j,l_2} \rangle}{\|\Lambda_{i,l_1}\| \Lambda_{i,1_1}\|}, \quad \text{for all } i \neq j. \tag{2}$$

The use of normalized correlation coefficients to calculate isolines is a very efficient and reliable method. The calculation of the contour is very sensitive to the noise of the image, and the error caused by the noise will be gradually enlarged into the initial model along with the wrong estimation of the contour, which will eventually lead to the wrong features of the reconstructed three-dimensional structure. In addition to the error caused by noise, there is an inevitable error. Since the image goes through a certain step size, the contour is obtained after discretization. The smaller the step size is, the more reliable the contour is, but there is still a small amount of error.

The basic principle of the angle reconstruction algorithm is to choose three different projection images, and use the equivalent line between them and the normal vector of the projection image to establish a rectangular coordinate system. In addition, the relative positions of other remaining surfaces can be determined by the isolines between each other, and the projection angles of all surfaces can be obtained. The specific algorithm process is as follows:

(1) The algorithm calculates the Euler angles α and β

The algorithm takes the projected images 1, 2, and 3 as examples to establish the coordinate system. First, the algorithm selects the equivalence line $\hat{C}_{12}$ of face 1 and face 2 on face 1 as the Z-axis. The expression for the equivalence line $\hat{C}_{ij}$ on face i and face j and lying on face i is usually

$$\hat{C}_{ij} = \begin{pmatrix} \sin\beta_{ij}\cos\alpha_{ij} \\ \sin\beta_{ij}\sin\alpha_{ij} \\ \cos\beta_{ij} \end{pmatrix}. \tag{3}$$

Since $\hat{C}_{12}$ is used as the Z-axis, the $\alpha_{12} = 0°$, $\beta_{12} = 0°$ of face 1, so the expression of the equivalent line $\hat{C}_{12}$ vector is

$$\hat{C}_{12} = \begin{pmatrix} 0 \\ 0 \\ 1 \end{pmatrix}. \tag{4}$$

Then, the algorithm chooses to place face 3 and face 1 and the equivalence line $\hat{C}_{31}$ on face 3 on the $Y-Z$ plane, then $\alpha_{31} = 90°$. Therefore, the normal vector of the plane 1 is parallel to the X-axis, and thus the three-dimensional coordinate system $X-Y-Z$ is fixed. Moreover, the v vector expression is

$$\hat{C}_{31} = \begin{pmatrix} 0 \\ \sin\beta_{31} \\ \cos\beta_{31} \end{pmatrix}. \tag{5}$$

For the equivalent line $\hat{C}_{23}$, the coordinates can be obtained as

$$\hat{C}_{23} = \begin{pmatrix} \sin\beta_{23}\cos\alpha_{23} \\ \sin\beta_{23}\sin\alpha_{23} \\ \cos\beta_{23} \end{pmatrix}. \tag{6}$$

Next the angle between the isolines can be calculated. Since $\hat{C}_{12}$ is the Z-axis direction vector, the following linear relationship can be obtained:

$$\cos A = \hat{C}_{31}\hat{C}_{12} = \cos\beta_{31}, \quad \cos B = \hat{C}_{12}\cdot\hat{C}_{23} = \cos\beta_{23}. \tag{7}$$

Moreover, we can also get

$$\cos C = \hat{C}_{23}\cdot\hat{C}_{32} = \sin\beta_{23}\cos\alpha_{23}\cdot\sin\beta_{31} + \cos\beta_{23}\cos\beta_{31}. \tag{8}$$

It is not difficult to see that the above equation is similar to the cosine rule for spherical trigonometry. Except for $\sin\alpha_{23}$, other values are known, and only by asking for this value, the exact values of the vectors

$\hat{C}_{12}$, $\hat{C}_{23}$, and $\hat{C}_{31}$ can be obtained. From the above equations, two correct but essentially different solutions of the equivalence line can be obtained, one is a left-handed combination and the other is a right-handed combination. The chirality of the combination of these three vectors can be determined by the determinant of the matrix composed of these three vectors. By combining $\hat{C}_{12}$, $\hat{C}_{23}$, and $\hat{C}_{31}$, we obtain

$$D = \begin{vmatrix} 0 & \sin\beta_{23}\cos\alpha_{23} & 0 \\ 0 & \sin\beta_{23}\sin\alpha_{23} & \sin\beta_{31} \\ 1 & \cos\beta_{23} & \cos\beta_{31} \end{vmatrix} = \sin\beta_{23}\cos\alpha_{23}\sin\beta_{31}. \tag{9}$$

After the equivalence line between the projected images is determined, the normal vectors $\hat{D}_1$, $\hat{D}_2$, and $\hat{D}_3$ of the image can be obtained by the outer product of the equivalence line vectors.

$$\hat{D}_1 \sim \hat{C}_{31} \times \hat{C}_{12}, \hat{D}_{21} \sim \hat{C}_{12} \times \hat{C}_{23}, \hat{D}_3 \sim \hat{C}_{23} \times \hat{C}_{31}. \tag{10}$$

From the above vectors, the Euler angles α and β of the projected image can be obtained.

(2) The algorithm calculates the γ angle in the Euler angle

The orientation angles of the different projected images determine how these images are rotated from their original 2D planar coordinates (the local coordinate system) into the 3D reconstructed coordinate system (the real coordinate system). At the beginning, $\hat{C}_{12}$ is set to the direction of the Z axis, and the projection angles γ_1 and γ_2 of face 1 and face 2 are also fixed accordingly. At this time, only the Euler angle γ_3 still needs to be determined. In order to find γ_3, it is necessary to calculate the coordinate value of the vector in the local coordinate system (that is, the two-dimensional coordinate system before being rotated to the reconstruction space, which can also be understood as the coordinate along the Z-axis when it is zero). This vector can be represented in real space as

$$\hat{C}_{31} = \begin{pmatrix} 0 \\ \sin\beta_{31} \\ \cos\beta_{31} \end{pmatrix}. \tag{11}$$

In order to get the expression of the vector in the local coordinate system, it is necessary to inversely rotate the vector back into the local coordinate system along the projection angles α and β of face 3 to obtain a new vector.

$$\begin{aligned} \hat{C}'_{31} &= \begin{pmatrix} \cos\beta_3\cos\alpha_3 & \cos\beta_3\sin\alpha_3 & -\sin\beta_3 \\ -\sin\alpha_3 & \cos\alpha_3 & 0 \\ \sin\beta_3\cos\alpha_3 & \sin\beta_3\sin\alpha_3 & \cos\beta_3 \end{pmatrix} \begin{pmatrix} 0 \\ \sin\beta_{31} \\ \cos\beta_{31} \end{pmatrix} \\ &= \begin{pmatrix} \cos\beta_3\sin\alpha_3\sin\beta_{31} - \sin\beta_3\cos\beta_{31} \\ \cos\alpha_3\sin\beta_{31} \\ \sin\beta_3\sin\alpha_3\sin\beta_{31} + \cos\beta_3\cos\beta_{31} \end{pmatrix}. \end{aligned} \tag{12}$$

At this time, the vector $\hat{C}_{31}$ does not contain the information of the angle γ_3 in the process of rotating back to the local coordinate system. Moreover, the above rotated vector is located on the X–Y plane, and the Z coordinate is zero. It can be assumed that the rotated coordinate is

$$\hat{C}'_{31} = \begin{pmatrix} \cos\theta \\ \sin\theta \\ 0 \end{pmatrix}. \tag{13}$$

The only parameter θ unknown so far can be derived from formula (13). In order to find the rotation angle γ_3 of face 3, the equivalent line vector in real space is rotated back to the two-dimensional plane of the original image according to the rotation angles α and β of face 3. Unable to calculate directly during rotation γ, that is, the difference between the equivalent line $\hat{C}_{31}$ in the local coordinate system and the real coordinate system is

the value of the rotation angle γ_3 generated by the face 3 when it enters the reconstruction space, that is, $\gamma_3 = \varphi - \theta$. Among them, the angle φ is the index value of the contour obtained when using the correlation to find the position of the contour.

2.2 Isometric screening based on voting algorithm

The angle reconstruction algorithm is very dependent on the reliability of the equivalence line. The error introduced by the equivalent line will be brought into the estimation process of the projection angle, and will be magnified in the result. Therefore, it is very important to obtain a reliable equivalent line to estimate the orientation angle of the projected image, and it is also one of the key steps to obtain a reliable three-dimensional structure. Image k_2 has a common equivalence line in space. According to the equivalence line, only the relative positions of the two images can be determined. They can be rotated along the equivalence line, but the relative position remains unchanged. When the third projected image is added, the equivalence lines between the three images can fix their positions, and then according to the equivalence lines between them and other images, the positions of all the projected images can be determined. Moreover, according to the equivalence line, the angle α_{12} between the first two images k_1 and k_2 can be calculated through the third projected image k_3. The projection image filtering algorithm proposed in this article mainly relies on the reliable equivalent line algorithm, so the angle calculation process will not be emphasized in detail here. This study only introduces the algorithm process of screening the equivalent line, as shown in Figure 3.

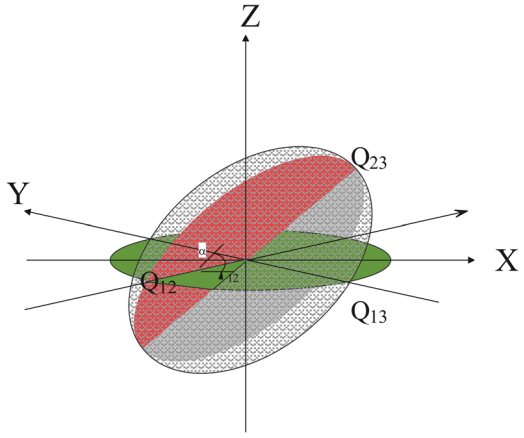

Figure 3: Schematic diagram of estimating the angle α_{12} between two projection images k_1 and k_2 based on the principle of angle reconstruction.

The angle between the known projected image and the projected image can be estimated by the third surface k_3 using the equivalence line between them.

2.3 Calibration of *y* angles in Euler angles and screening of projected images

The main problem of 3D reconstruction in teaching monitoring based on angle reconstruction method is how to obtain the projection angle information from the sample image information whose projection direction is unknown. Since the sample particles are projected to produce a two-dimensional image, in order to avoid the destruction of the particle structure by electrons, a lower power is used, which makes the projected image

obtain a lower signal-to-noise ratio. High noise brings more obstacles to the process of obtaining the contour. This study proposes a new algorithm to calibrate the projection angle γ based on the principle of angle reconstruction. The basic principle is that for a certain image, every other image can be used to estimate a γ value of the image. Then, these gamma values are averaged to calibrate the original γ value.

(1) The calculation process of Euler angle γ is as follows:

Taking projected image i and projected image j as examples, this study knows α_i, β_i, and γ_i of face i, α_j and β_j of face j, and find γ_j of projected face j.

For projected image i and projected image j, the expression of the equivalent line vector of face i and face j and on face i in the original coordinate system (that is, in the X–Y plane) is

$$\hat{C}_{ij} = \begin{pmatrix} \cos\varphi_i \\ \sin\varphi_i \\ 0 \end{pmatrix}. \tag{14}$$

Among them, φ_i is the index value of the equivalence line of the projected image i and the projected image j on the image i. The rotation matrix of $\hat{C}_{ij}$ from the original coordinate system to the real space is

$$R_i = R_{\gamma_i} R_{\beta_i} R_{\alpha_i} = \begin{pmatrix} \cos\gamma_i & \sin\gamma_i & 0 \\ -\sin\gamma_i & \cos\gamma_i & 0 \\ 0 & 0 & 1 \end{pmatrix} \begin{pmatrix} \cos\beta_i & 0 & -\sin\beta_i \\ 0 & 1 & 0 \\ \sin\beta_i & 0 & \cos\beta_i \end{pmatrix} \begin{pmatrix} \cos\alpha_i & \sin\alpha_i & 0 \\ -\sin\alpha_i & \cos\alpha_i & 0 \\ 0 & 0 & 1 \end{pmatrix}. \tag{15}$$

Therefore, in real space, the direction of the isoline vector between faces i and j on the projected image i lies in the real space as shown in formula (16)

$$C_{ij} = R_i \begin{pmatrix} \cos\varphi_i \\ \sin\varphi_i \\ 0 \end{pmatrix}. \tag{16}$$

After the above rotation, we have obtained the equivalent line vector located on the face i in the real space, and then we need to rotate the vector along the projection angles α_j and β_j of the face j to the original local space of the face j. The rotation vector formed by α_j and β_j is

$$R_j = R_{\beta_j} R_{\alpha_j}. \tag{17}$$

The rotated vector is

$$\hat{C}'_{ji} = R_j C_{ij} \begin{pmatrix} \cos\beta_j & 0 & -\sin\beta_j \\ 0 & 1 & 0 \\ \sin\beta_j & 0 & \cos\beta_j \end{pmatrix} \begin{pmatrix} \cos\alpha_j & \sin\alpha_j & 0 \\ -\sin\alpha_j & \cos\alpha_j & 0 \\ 0 & 0 & 1 \end{pmatrix} C_{ij} = \begin{pmatrix} \cos\theta \\ \sin\theta \\ 0 \end{pmatrix}. \tag{18}$$

The angle between the vector $\hat{C}'_{ji}$ and the vector $\hat{C}_{ij}$ is the Euler angle γ_j of the desired projection surface j. Moreover, both the angle θ and the angle φ_j are already known numbers, and from this, $\gamma_j = (\varphi_j - \theta)$ can be obtained. Among them, φ_j is the index value of the equivalent line of the projection surface i and the surface j and located on the surface j.

The above is the specific algorithm process of using one projection surface to find the Euler angle γ of another projection surface. The diagrammatic process is shown in Figure 4.

(2) After the calculation process of Euler angles is known, the γ-angle of each projection surface can be calibrated. The specific method is as follows:

We assume that there are N projection images, choose one image i, and use the remaining $N-1$ images to calculate the γ angle of image i, then we can get $N-1$ different values, and take the average of these values. The calculation formula is as follows:

$$\bar{\gamma} = \sum_{j=1,\ldots,N \text{ and } j\neq i} \gamma_j. \tag{19}$$

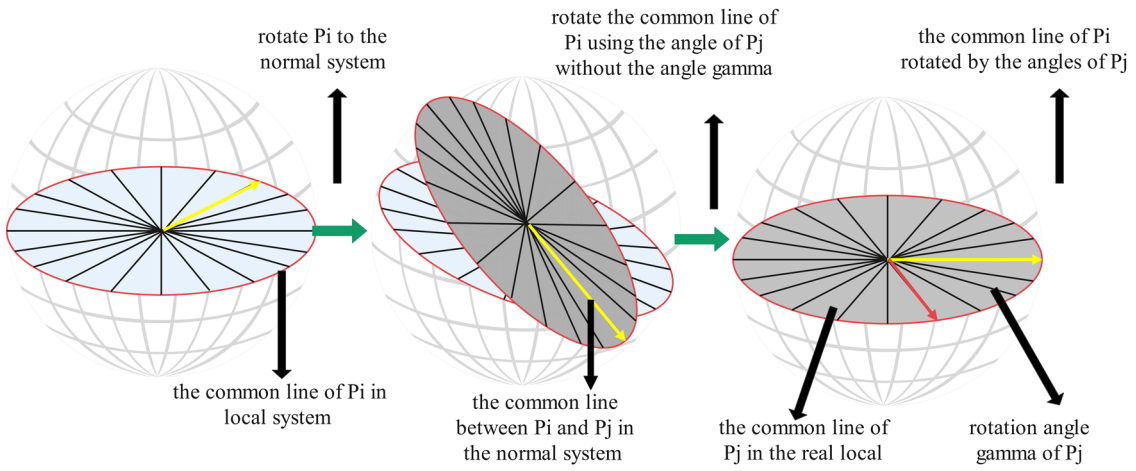

Figure 4: The calculation process of the projection angle γ.

The average value is used to replace the original γ value of image i, and so on, and the average value of the γ value of N images is replaced to complete a calibration. Then, the algorithm iteratively and repeatedly calculates the above process, and stops when the value of the γ angle of each image tends to be stable.

The blue surface represents surface i, and the yellow line segment represents the equivalent line of surface i. At this time, the common intersection line of the surface j represented by the yellow surface and the surface i in the real space is the equivalence line, that is, the equivalence line of the surface j at this time, that is, the red line segment coincides with the yellow line segment. Next we rotate the yellow line segment along the α, β angle of face j back to the original local space of face j. At this time, the angle between the yellow line segment and the red line segment is the γ angle of face j.

3 Results

It can be seen from Figure 5 that the peaks of these groups of statistical graphs are high and low, and the results with higher peaks often represent that the Euler angle calculation of the corresponding image is also more accurate. On the contrary, if there is a large error in the projection angle of the image, the value distribution of the obtained γ angle will be more scattered, which means that the graph is wider and the peak value is lower in the histogram. The reason is that the projection angle of the image with lower quality

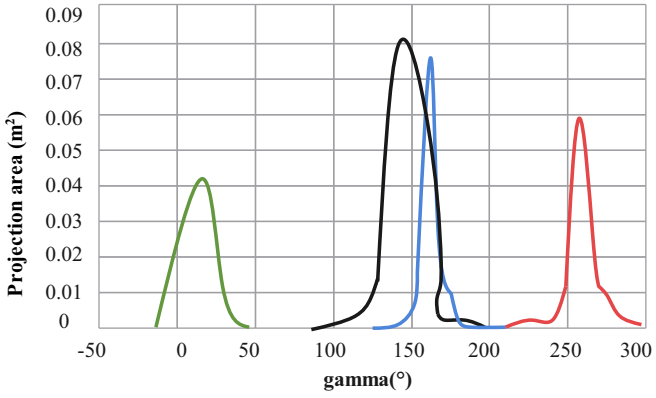

Figure 5: Histogram statistics of the calculation results of the γ angle of four groups of different projection surfaces.

often has a larger error, and the obtained γ angle error will also be relatively large, resulting in a large difference between the calculation results of different projection images, and the data distribution is not concentrated.

On the basis of the above research, the construction of the online teaching quality evaluation system in colleges and universities is carried out. The functional module design of the system is shown in Figure 6.

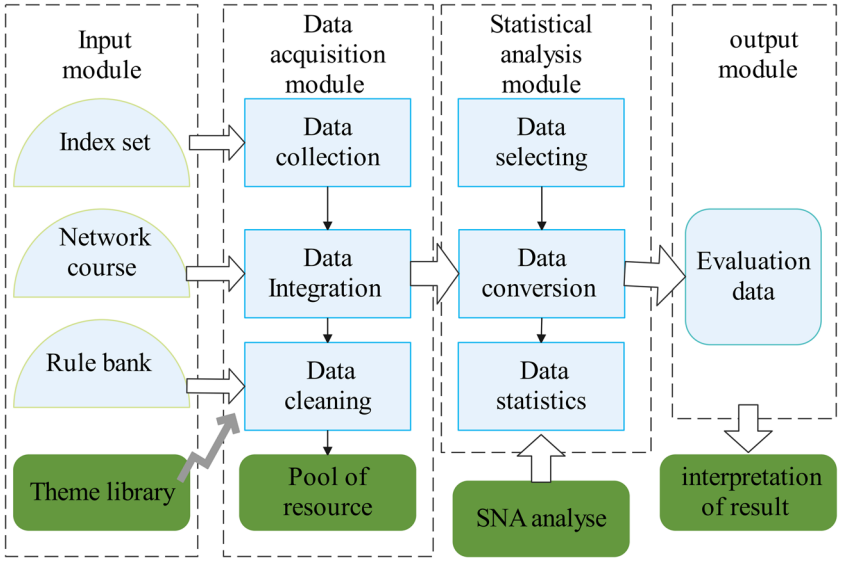

Figure 6: Design of system functional modules.

The online classroom state monitoring system is mainly composed of three modules, the login module, the student class process detection module, and the classroom state assessment module. Its overall design is shown in Figure 7.

Figure 8 shows an image example of real-time monitoring of students in online teaching in this study.

This study verifies the effect of the online teaching quality evaluation system in colleges and universities based on digital monitoring technology proposed in this work. Moreover, this study uses network teaching to collect multiple sets of image and video data, verifies the effect of the online teaching monitoring system, and counts the effect of online teaching monitoring, and obtains the results shown in Table 1 and Figure 9.

Through evaluation experiments (Table 1), the effectiveness of the online teaching quality evaluation system for universities based on digital monitoring technology was verified. From the evaluation results, it can be seen that the evaluation results of the system model in this study are distributed between [84,92], indicating that the use of the system in this work is very excellent.

4 Analysis and discussion

In the process of teaching and monitoring 3D reconstruction, the main purpose is to arrange the images and their projection angles in their respective positions in Fourier space to complete the reconstruction. Therefore, the quality of the projected image and the accuracy of the projection angle have a great influence on the reconstruction effect. The reason is not only that the high noise of the image causes the estimation deviation of the equivalence line and the projection angle, but also causes the initial model to have wrong features due to factors such as wrong features in the image. Therefore, in the process of constructing the initial model, if those low-quality projection images or whose projection angles cannot be accurately estimated can be effectively screened out, the accuracy of the initial model can be greatly enhanced.

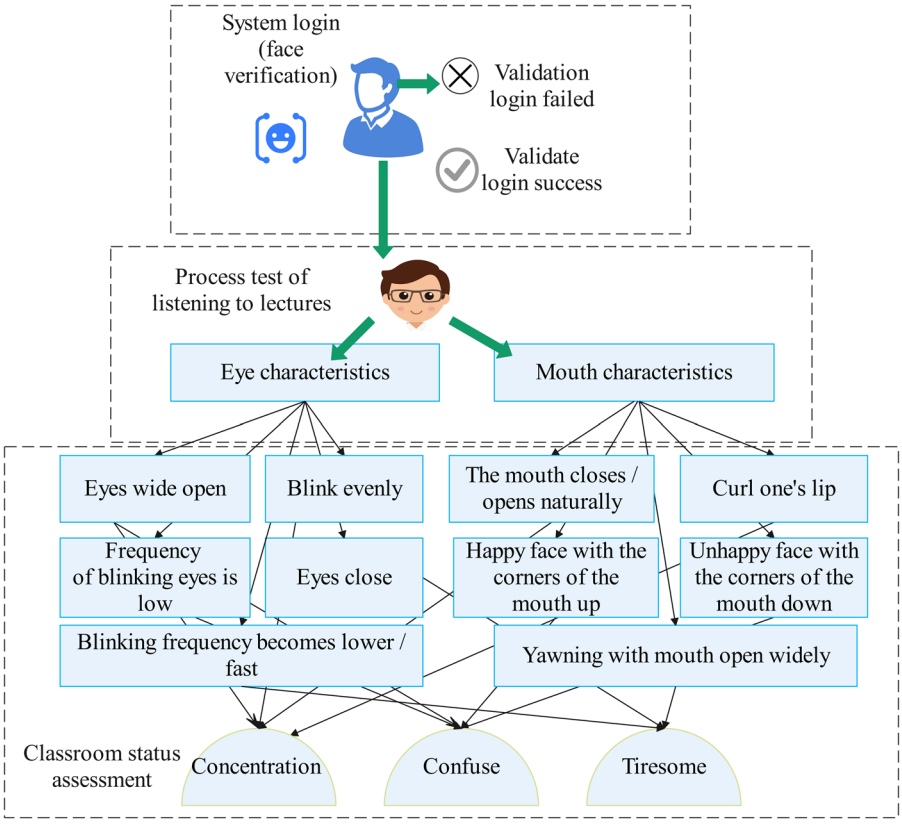

Figure 7: Online teaching monitoring system.

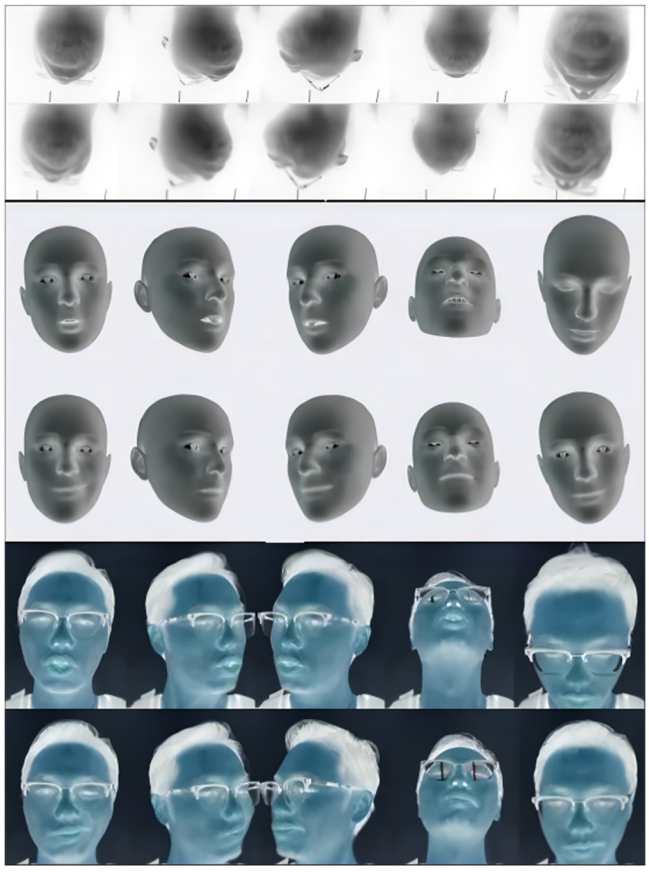

Figure 8: Image example of real-time monitoring of students in online teaching.

Table 1: Monitoring effect of online teaching

Num	Monitoring accuracy (%)	Num	Monitoring accuracy (%)	Num	Monitoring accuracy (%)
1	89.15	15	84.42	28	84.80
2	90.48	16	91.92	29	84.89
3	90.75	17	86.49	30	91.13
4	87.81	18	88.43	31	91.97
5	92.16	19	92.90	32	85.17
6	86.46	20	86.79	33	91.26
7	86.07	21	92.89	34	86.14
8	88.54	22	90.35	35	86.96
9	88.50	23	91.15	36	87.38
10	90.55	24	89.19	37	90.91
11	89.49	25	88.67	38	91.38
12	85.44	26	89.18	39	86.58
13	84.03	27	92.75	40	84.72
14	90.07				

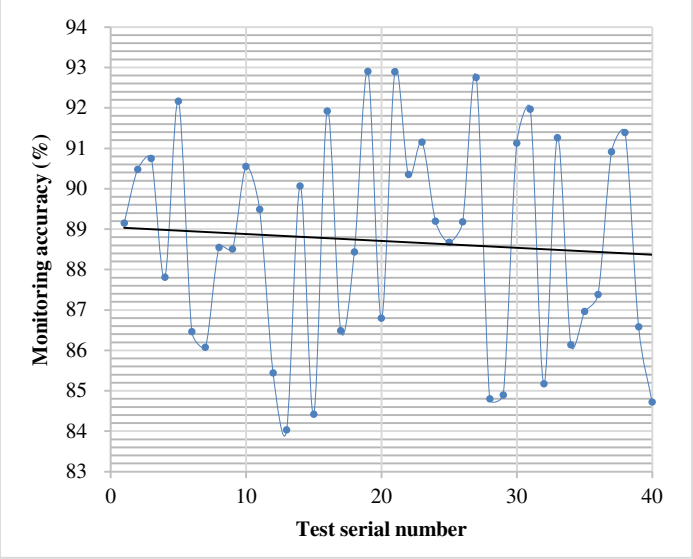

Figure 9: Statistical diagram of teaching monitoring effect.

Screening projected images based on Euler angles γ is the core algorithm in this work. After experimental verification, the algorithm can effectively judge the quality of the projection image, and the initial model constructed by screening out the projection images with lower quality is significantly improved compared to the initial model constructed by the projection images without screening.

In the process of calibrating the Euler angle γ, we found that the angle γ is very sensitive to the changes in the projection angles α and β of the image, that is, by calculating the angle γ, the correctness of the remaining two directional angles can be judged. In the process of using the projection image to find the γ angle, the γ of some images is calibrated and the error is larger. The reason is that the rotation angles α and β of the image itself have a large deviation, so no matter how other projection images calculate the γ angle of the image, the calculation cannot be accurate, and the calculated results have great discreteness. However, for those images with more intensive calculation results, their α and β angles have higher reliability.

Through evaluation experiments, the effectiveness of the online teaching quality evaluation system for universities based on digital monitoring technology was verified. From the evaluation results, it can be seen

that the evaluation results of the system model in this study are distributed between [84,92], indicating that the use of the system in this study is very excellent.

It can be seen from the experimental research that the digital online monitoring technology proposed in this work can monitor students in real time in online teaching in colleges and universities, effectively improve the participation of students in the online teaching process, and play an important role in improving the quality of teaching.

5 Conclusion

When students' emotions and behaviors are against the learning class, teachers are often unable to correct and give reminders in time, resulting in greatly reduced students' learning effects. Therefore, around the above problems in online classrooms, this work makes a detailed study on the online classroom status monitoring system based on facial expression analysis. Moreover, in view of the problems existing in the online classroom, this study proposes a digital online teaching monitoring technology to evaluate the classroom status from the face detection, face recognition, facial features, and other aspects of students. In addition, this work practices an online classroom state monitoring system based on facial expression analysis. The experimental research shows that the digital online monitoring technology proposed in this study can monitor students in real time in online teaching in colleges and universities, effectively improve the participation of students in the online teaching process, and play an important role in improving the quality of teaching.

This study does not classify emotions in detail in the process of emotion recognition and verification. In the future work, we can specifically identify students' weariness and other emotions, which is also where the digital teaching monitoring system needs to be improved in the next step.

The projection image filtering algorithm based on Euler angles can filter out low-quality projection images, which also includes projection images that are considered low-quality due to inaccurate estimation of projection angles. So, in future research, we can correct the projection angle of this part of the image. By using the projection angles of higher quality projection images to re-estimate the Euler angle α of lower quality projection images, β and γ, the modified projection image can be retained for the construction of the initial model.

Funding information: This study was supported by "Ningxia Key Research and Development Plan (Special Project for Talent Introduction) in 2022, Project number: 2022BSB03049." Ningxia Key R&D Plan project: Development and application research of Minning Education Cooperation Platform based on "Internet +", project number: 2023BEG03064.

Author contributions: Conceptualization, Wanzhi Ma; Methodology, Wanzhi Ma; Software, Na Chu, Validation, Na Chu; Formal Analysis, Na Chu; Investigation, Na Chu; Resources, Na Chu; Data Curation, Na Chu; Writing – Original Draft Preparation, Wanzhi Ma; Writing – Review & Editing, Na Chu.

Conflict of interest: The authors declare that they have no conflicts of interest to report regarding the present study.

Data availability statement: The datasets generated during and/or analysed during the current study are available from the corresponding author on reasonable request.

References

[1] Vargo D, Zhu L, Benwell B, Yan Z. Digital technology use during COVID-19 pandemic: A rapid review. Hum Behav Emerg Technol. 2021;3(1):13–24.

[2] Han L. Teaching exploration and practice of innovative practical course configuration monitoring technology. Adult High Educ. 2022;4(1):30–7.
[3] Esteve-Mon FM, Llopis-Nebot MÁ, Adell-Segura J. Digital teaching competence of university teachers: A systematic review of the literature. IEEE Rev Iberoam de Tecnol del Aprendiz. 2020;15(4):399–406.
[4] Hromalik CD, Koszalka TA. Self-regulation of the use of digital resources in an online language learning course improves learning outcomes. Distance Educ. 2018;39(4):528–47.
[5] Cooper G, Park H, Nasr Z, Thong LP, Johnson R. Using virtual reality in the classroom: preservice teachers' perceptions of its use as a teaching and learning tool. Educ Media Int. 2019;56(1):1–13.
[6] Moorhouse BL, Wong KM. Blending asynchronous and synchronous digital technologies and instructional approaches to facilitate remote learning. J Computers Educ. 2022;9(1):51–70.
[7] Arnò S, Galassi A, Tommasi M, Saggino A, Vittorini P. State-of-the-art of commercial proctoring systems and their use in academic online exams. Int J Distance Educ Technol. 2021;19(2):55–76.
[8] Greenhow C, Lewin C, Staudt Willet KB. The educational response to Covid-19 across two countries: a critical examination of initial digital pedagogy adoption. Technol Pedagogy Educ. 2021;30(1):7–25.
[9] Bayanov DI, Novitskaya LY, Panina SA, Paznikova ZI, Martynenko EV, Ilkevich KB, et al. Digital technology: Risks or benefits in student training. J Environ Treat Tech. 2019;7(4):659–63.
[10] Rapanta C, Botturi L, Goodyear P, Guàrdia L, Koole M. Online university teaching during and after the Covid-19 crisis: Refocusing teacher presence and learning activity. Postdigital Sci Educ. 2020;2(3):923–45.
[11] Herodotou C, Hlosta M, Boroowa A, Rienties B, Zdrahal Z, Mangafa C. Empowering online teachers through predictive learning analytics. Br J Educ Technol. 2019;50(6):3064–79.
[12] Callo EC, Yazon AD. Exploring the factors influencing the readiness of faculty and students on online teaching and learning as an alternative delivery mode for the new normal. Univers J Educ Res. 2020;8(8):3509–18.
[13] Fletcher J, Everatt J, Mackey J, Fickel LH. Digital technologies and innovative learning environments in schooling: A New Zealand experience. New Zealand J Educ Stud. 2020;55(1):91–112.
[14] Reamer FG. Social work education in a digital world: Technology standards for education and practice. J Soc Work Educ. 2019;55(3):420–32.
[15] Gao K, Han F, Dong P, Xiong N, Du R. Connected vehicle as a mobile sensor for real time queue length at signalized intersections. Sensors. 2019;19(9):2059.
[16] Wang X, Li Q, Pan Y. Ant colony optimization-based location-aware routing for wireless sensor networks. International Conference on Wireless Algorithms, Systems, and Applications; 2008.
[17] Jiang Y, Tong G, Yin H, Xiong N. A pedestrian detection method based on genetic algorithm for optimize XGBoost training parameters. IEEE Access. 2019;7:118310–21.
[18] Wan R, Xiong N. An energy-efficient sleep scheduling mechanism with similarity measure for wireless sensor networks. Human-Centric Comput Inf Sci. 2018;8(1):1–22.
[19] Lu Y, Wu S, Fang Z, Xiong N, Yoon S, Park DS. Exploring finger vein based personal authentication for secure IoT. Future Gener Computer Syst. 2017;77:149–60.
[20] Yu L. The construction of a smart education system in colleges and universities based on cloud-side collaborative computing task scheduling algorithm. J Sens. 2022;2022:65–78.